Supporting Information

An electrophilic fragment screening for the development of small molecules targeting caspase-2

Matthew E. Cuellar[a,+], Mu Yang[a], Surendra Karavadhi[b], Ya-Qin Zhang[b], Hu Zhu[b], Hongmao Sun[b], Min Shen[b], Matthew D. Hall[b], Samarjit Patnaik[b], Karen H. Ashe[c], Michael A. Walters[a,*], and Steffen Pockes[a,d,*]

[a]Department of Medicinal Chemistry, Institute for Therapeutics Discovery and Development, University of Minnesota, Minneapolis, MN 55414, USA

[b]National Center for Advancing Translational Sciences, National Institutes of Health, Rockville, Maryland 20850, USA

[c]Department of Neurology, University of Minnesota, 2101 6th Street SE, Minneapolis, MN 55455, USA

[d]Institute of Pharmacy, University of Regensburg, Universitätsstraße 31, 93053 Regensburg, Germany

Corresponding authors: mwalters@umn.edu **(Michael A. Walters),** steffen.pockes@ur.de **(Steffen Pockes)**

Content

1. Distribution of physicochemical properties of the chloroacetamide library S3
2. Hit fragments from two-point dose screening at caspase-2 ..... S8
3. Fluorometric enzyme assay at Casp2 and Casp3 ..... S13
4. Target engagement study using MSPS S17
5. GSH-Glo™ Glutathione and CellTiter-Glo™ Luminescent Cell Viability Assay S22
6. Synthesis for hit validation S25
7. NMR spectra and RP-HPLC chromatograms of **97*** and **1269*** S27
8. References S31

1. Distribution of physicochemical properties of the chloroacetamide library

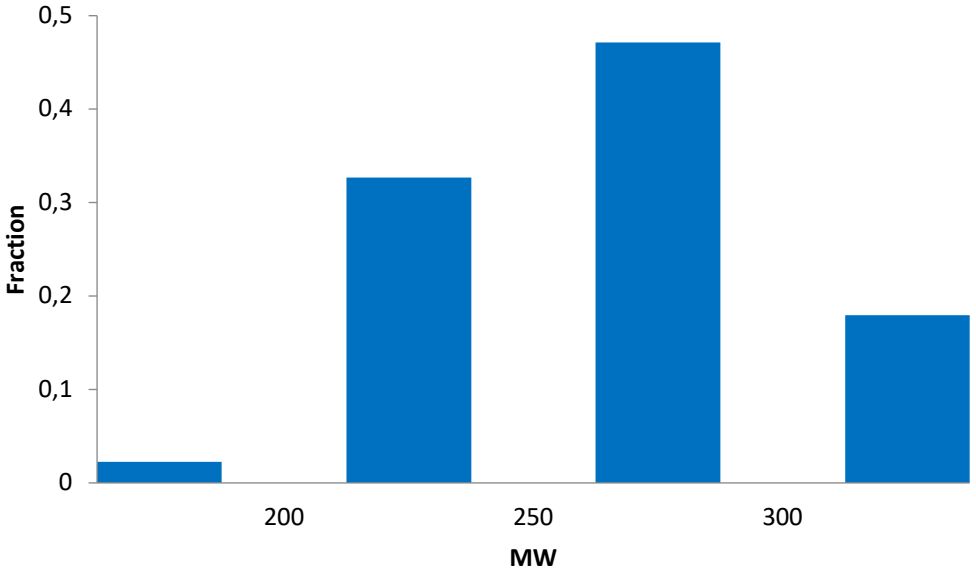

Figure S1. Distribution of molecular weight (MW) of the chloroacetamide library (1920 compounds) from Enamine.

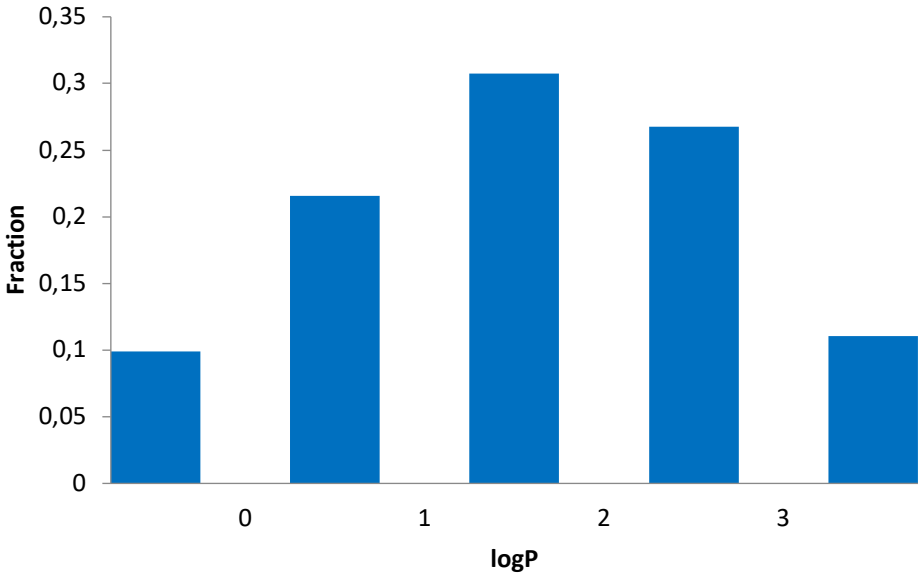

Figure S2. Distribution of logP of the chloroacetamide library (1920 compounds) from Enamine.

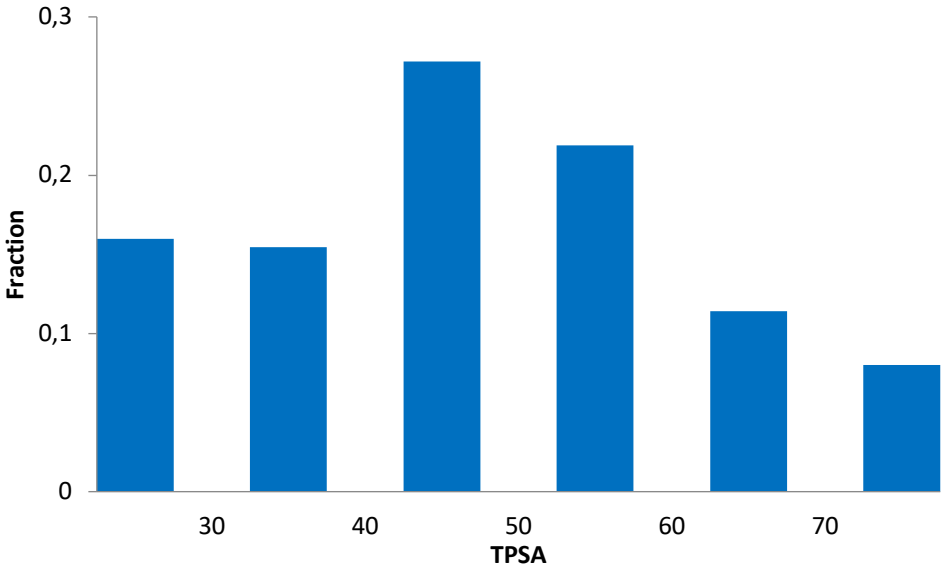

Figure S3. Distribution of topological polar surface area (TPSA) of the chloroacetamide library (1920 compounds) from Enamine.

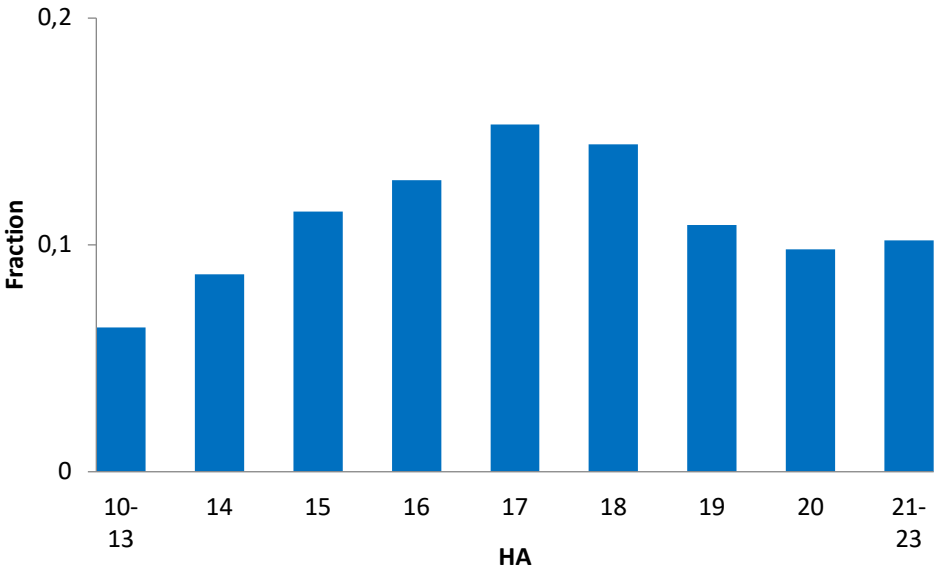

Figure S4. Distribution of heavy atoms (HA) of the chloroacetamide library (1920 compounds) from Enamine.

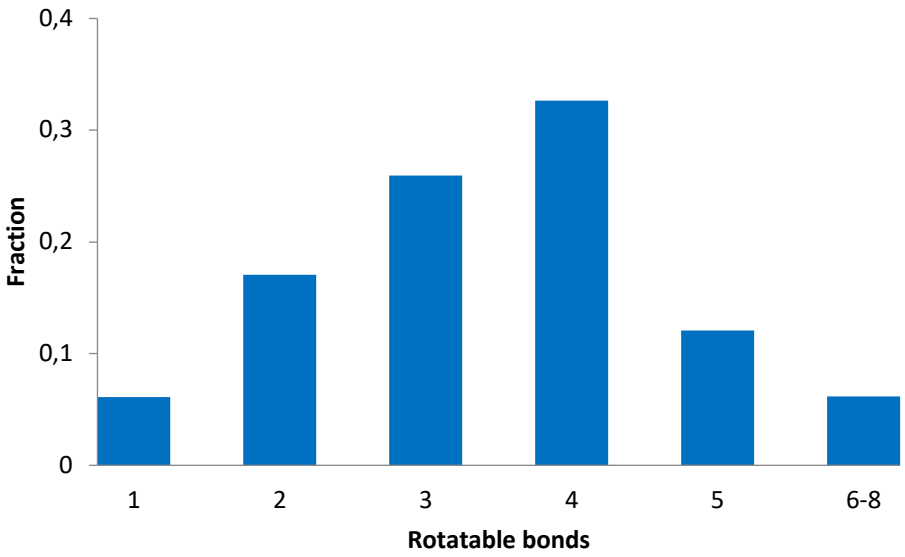

Figure S5. Distribution of rotable bonds of the chloroacetamide library (1920 compounds) from Enamine.

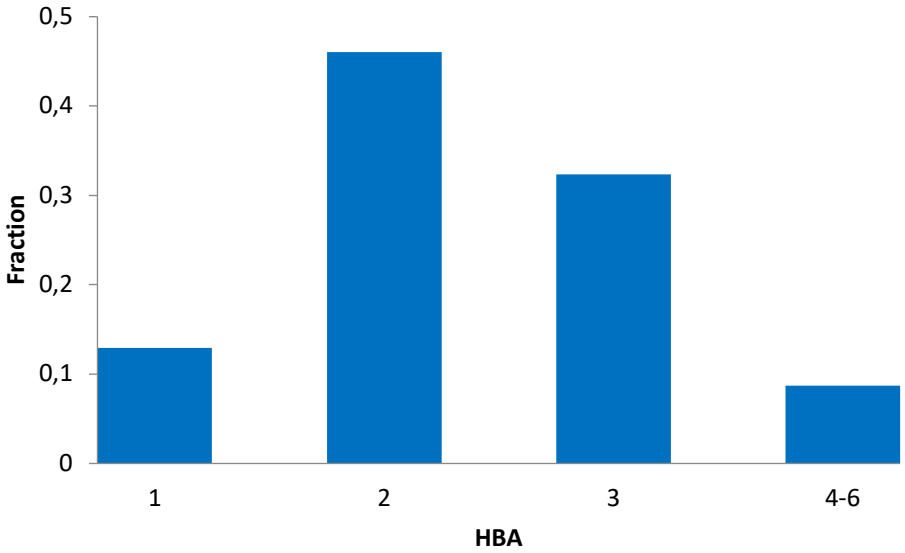

Figure S6. Distribution of H bond acceptors of the chloroacetamide library (1920 compounds) from Enamine.

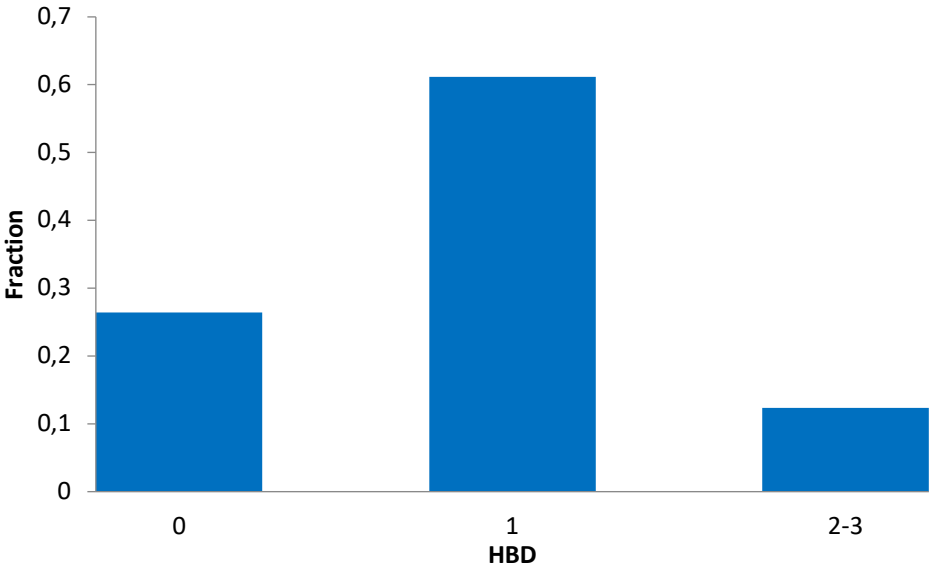

Figure S7. Distribution of H bond donors of the chloroacetamide library (1920 compounds) from Enamine.

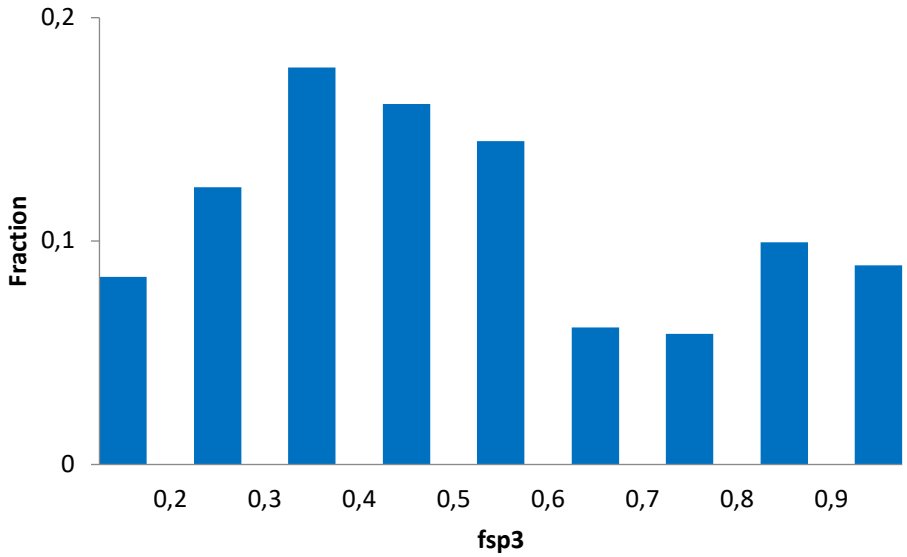

Figure S8. Distribution of fraction of sp^3 carbon atoms (fsp3) of the chloroacetamide library (1920 compounds) from Enamine.

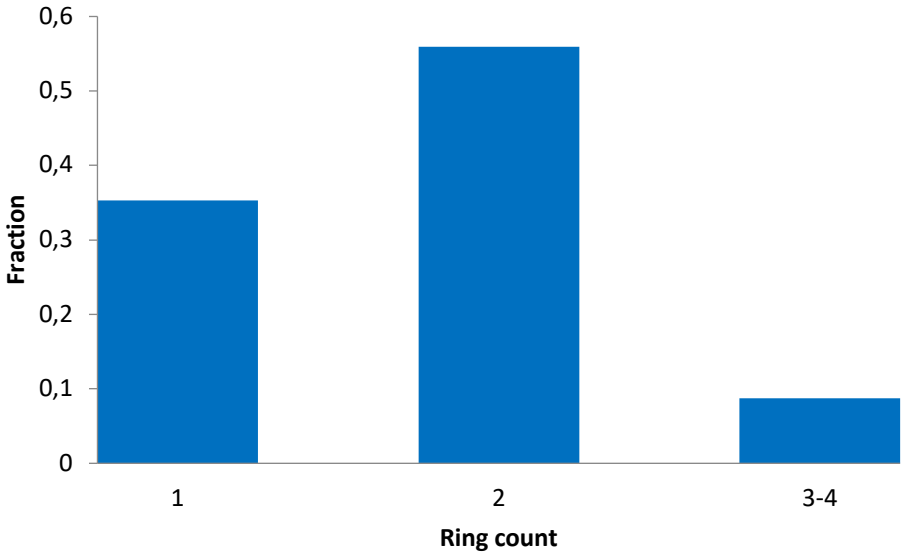

Figure S9. Distribution of ring count of the chloroacetamide library (1920 compounds) from Enamine.

2. Hit fragments from two-point dose screening at caspase-2

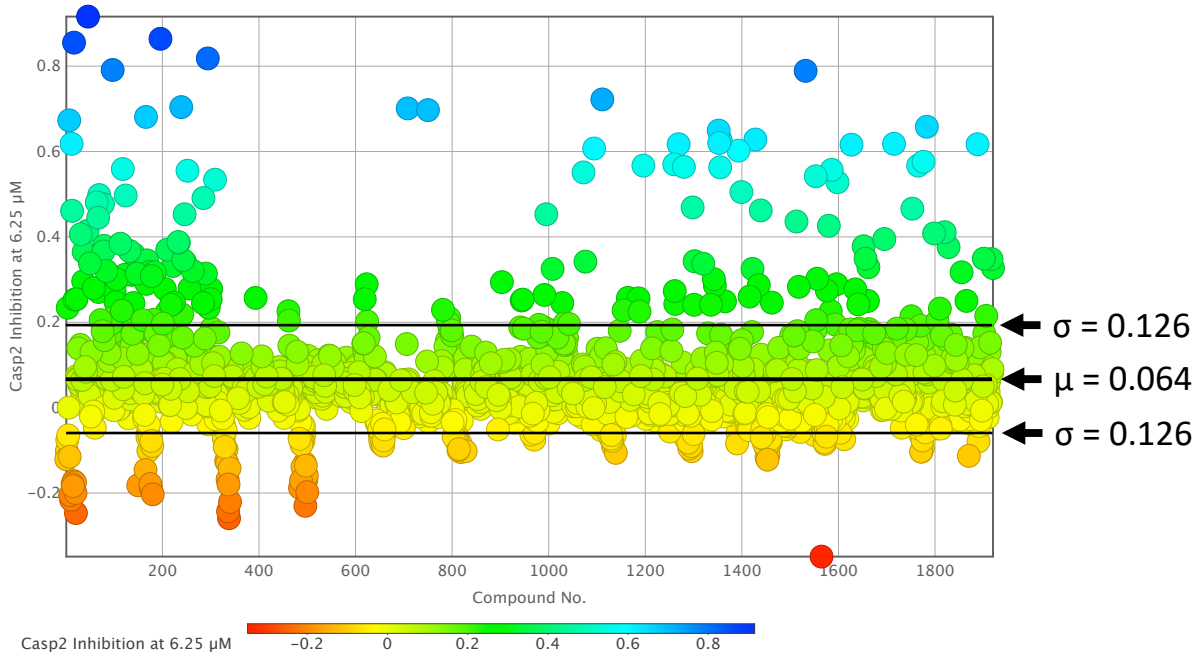

Figure S10. Caspase-2 inhibition plot of the two-point dose screening assay of compounds **1-1920** at 6.25 µM.

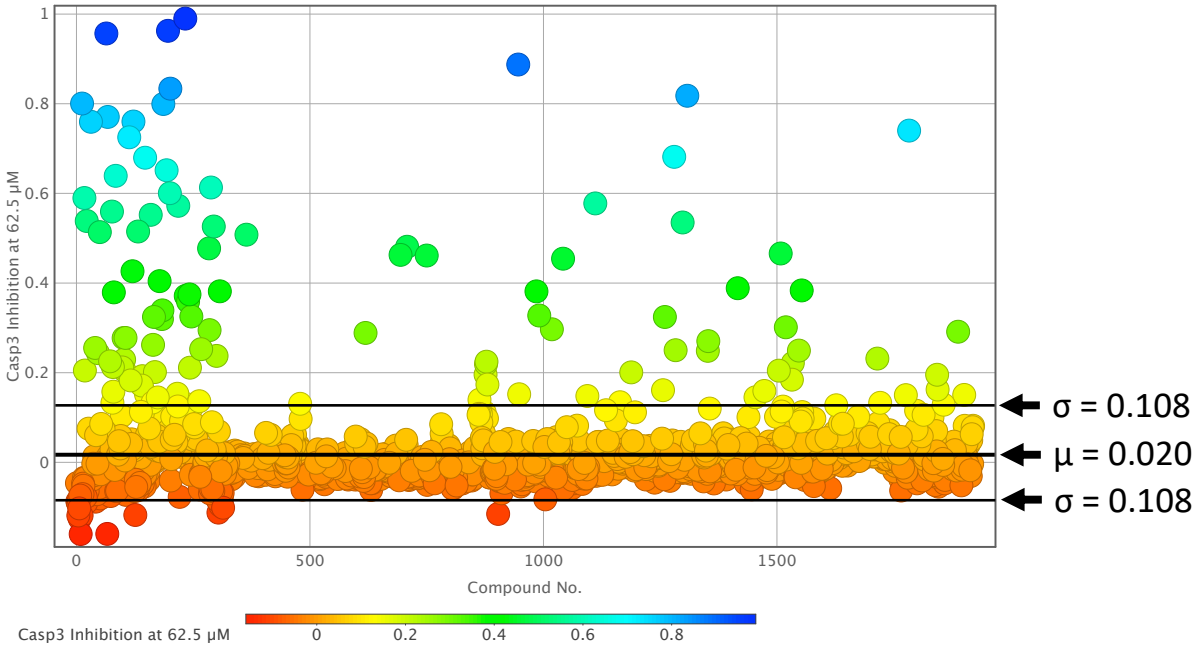

Figure S11. Caspase-3 inhibition plot of the two-point dose screening assay of compounds **1-1920** at 62.5 µM.

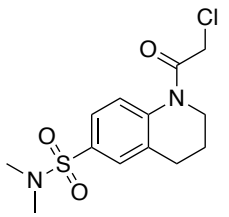

12

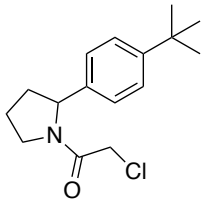

13

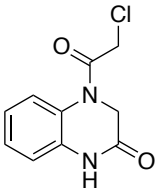

17

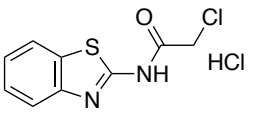

18

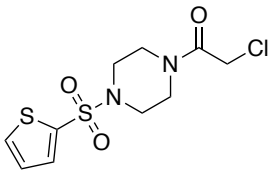

31

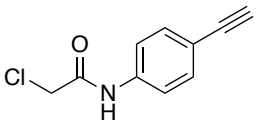

45

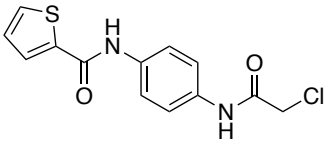

46

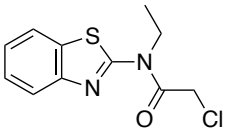

67

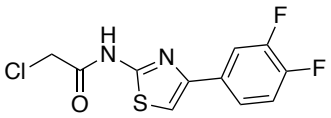

69

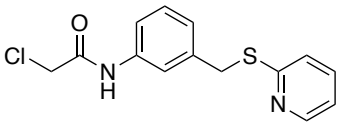

77

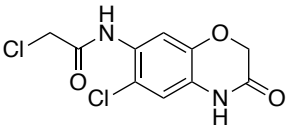

78

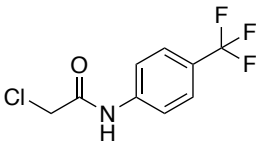

79

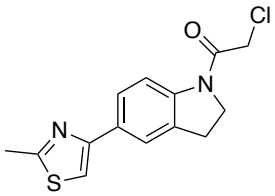

97

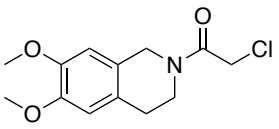

113

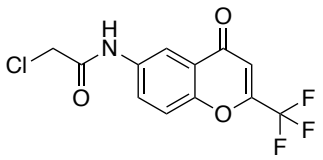

118

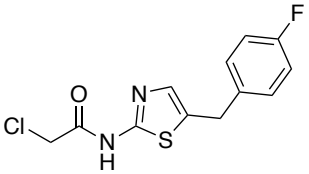

124

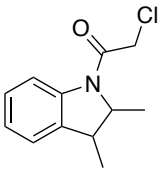

132

(continuation Figure S12)

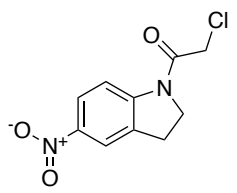

166

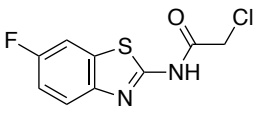

178

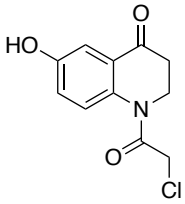

196

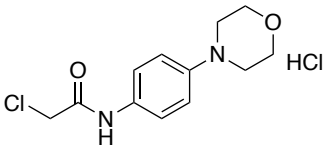

210

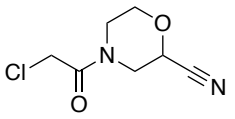

234

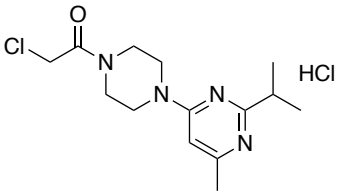

239

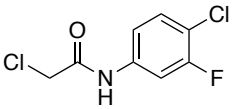

246

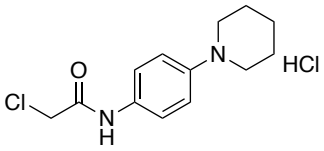

252

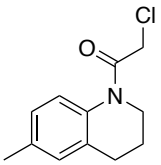

285

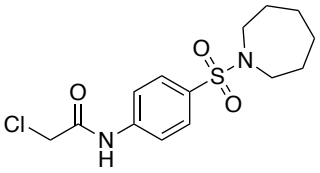

294

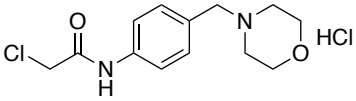

309

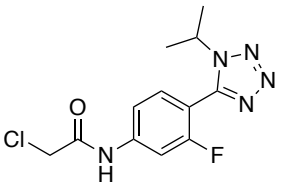

708

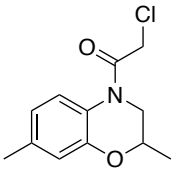

750

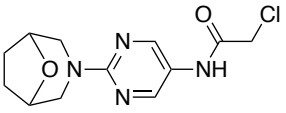

995

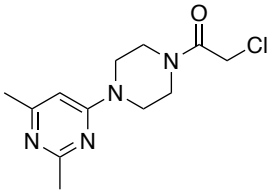

1072

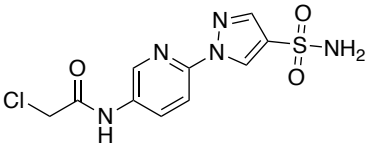

1094

(continuation Figure S12)

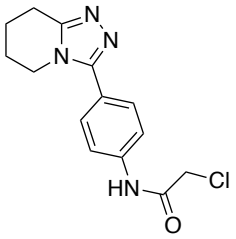

1111

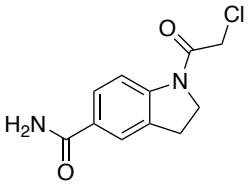

1196

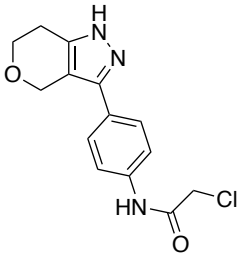

1260

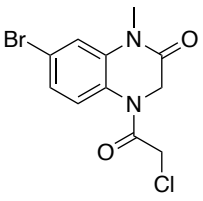

1269

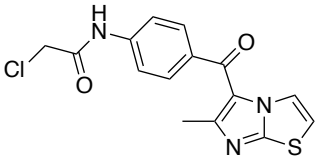

1280

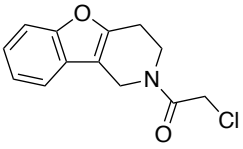

1298

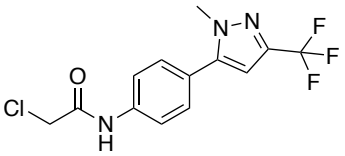

1352

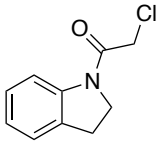

1353

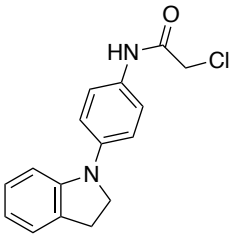

1355

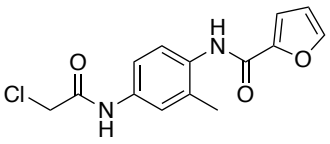

1356

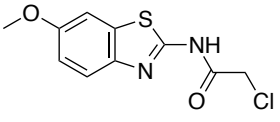

1393

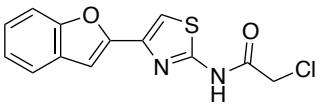

1399

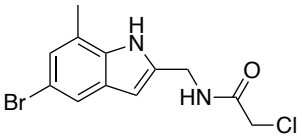

1428

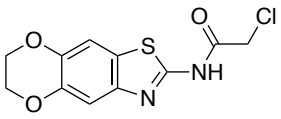

1439

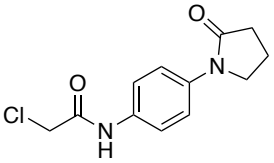

1513

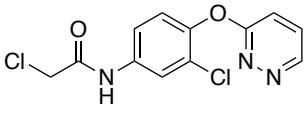

1532

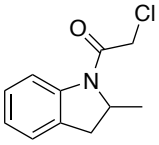

1553

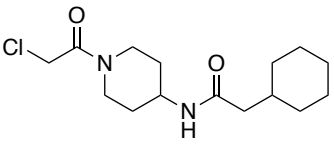

1580

(continuation Figure S12)

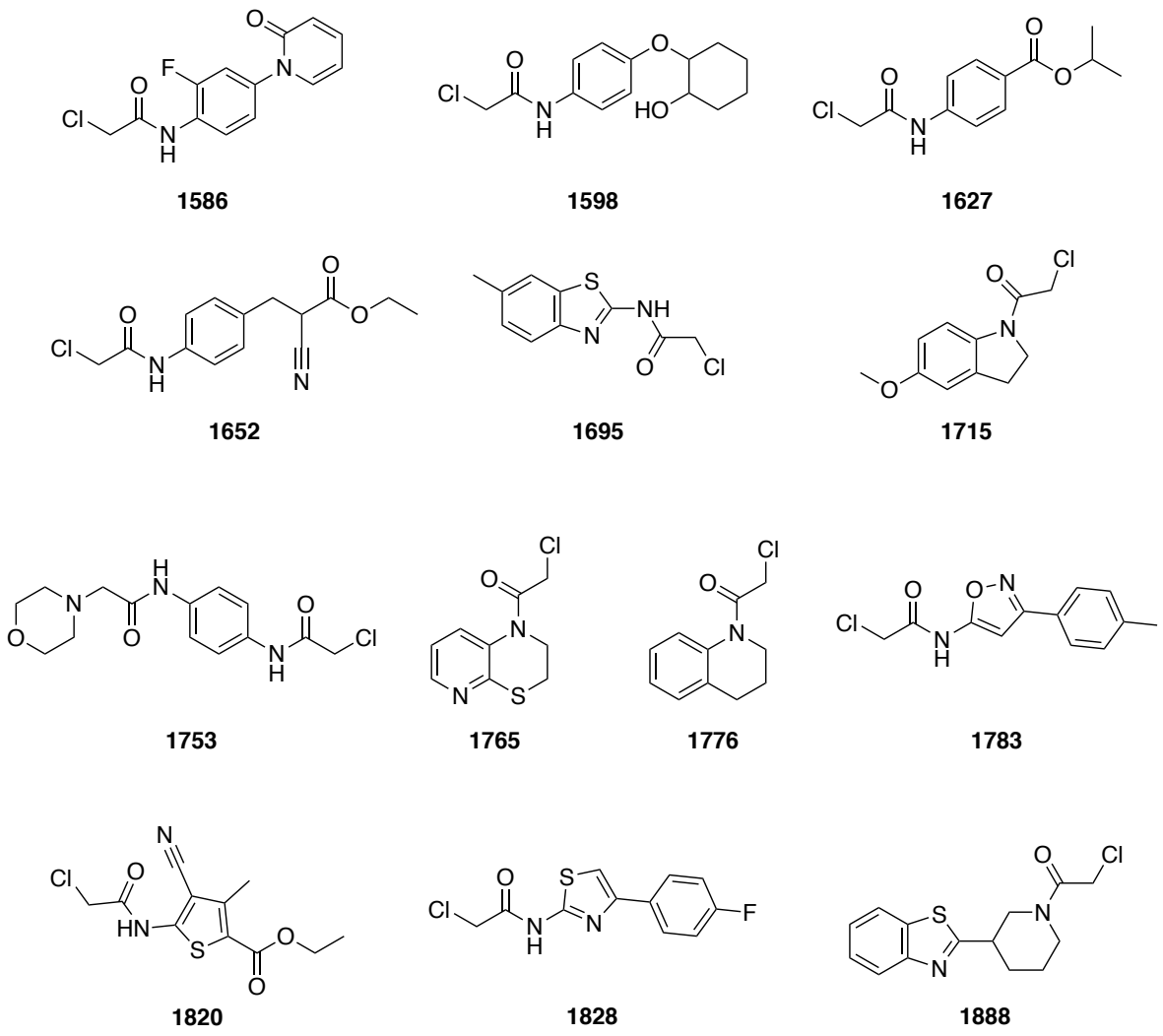

Figure S12. Chemical structures of 64 selected α-chloroacetamide hit fragments from two-point dose screening at Casp2.

3. Fluorometric enzyme assay at Casp2 and Casp3

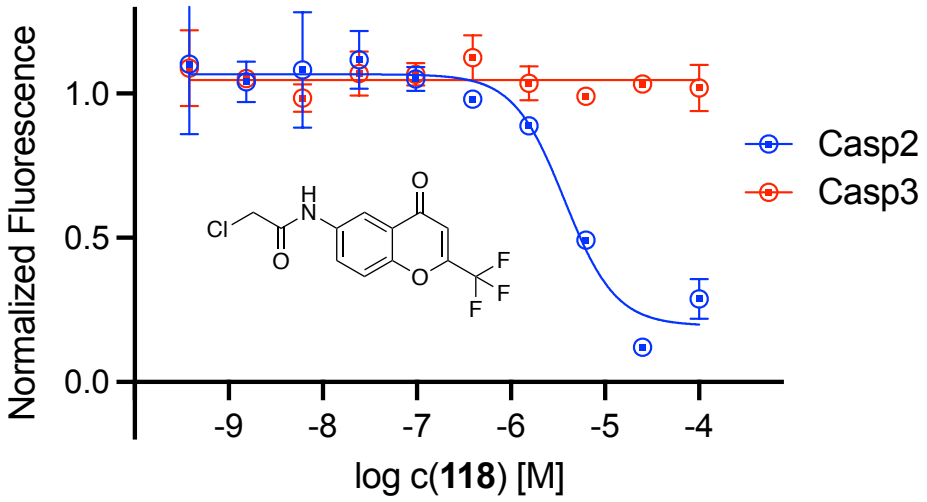

Figure S13. Concentration-response curve of **118** at caspase-2 (blue) and caspase-3 (red) in the fluorometric enzyme assay. Data points represent mean values ± SD from representative experiments, each performed in duplicate.

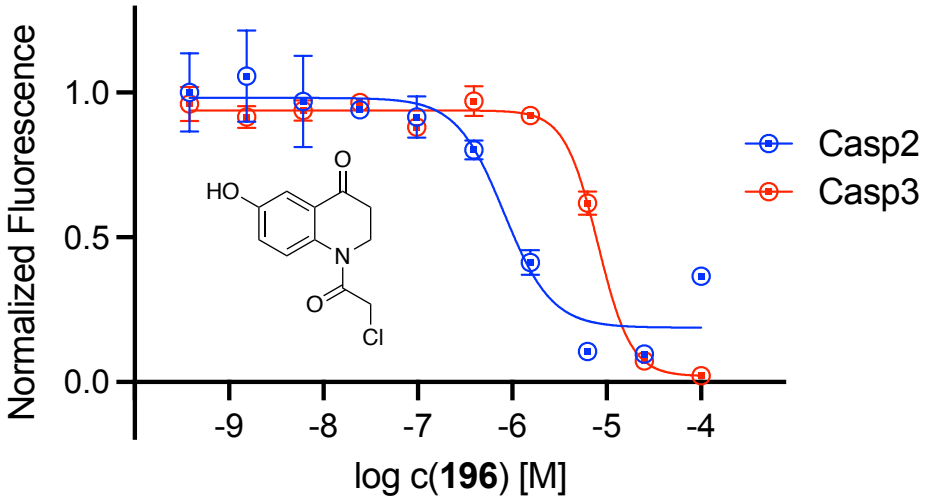

Figure S14. Concentration-response curve of **196** at caspase-2 (blue) and caspase-3 (red) in the fluorometric enzyme assay. Data points represent mean values ± SD from representative experiments, each performed in duplicate.

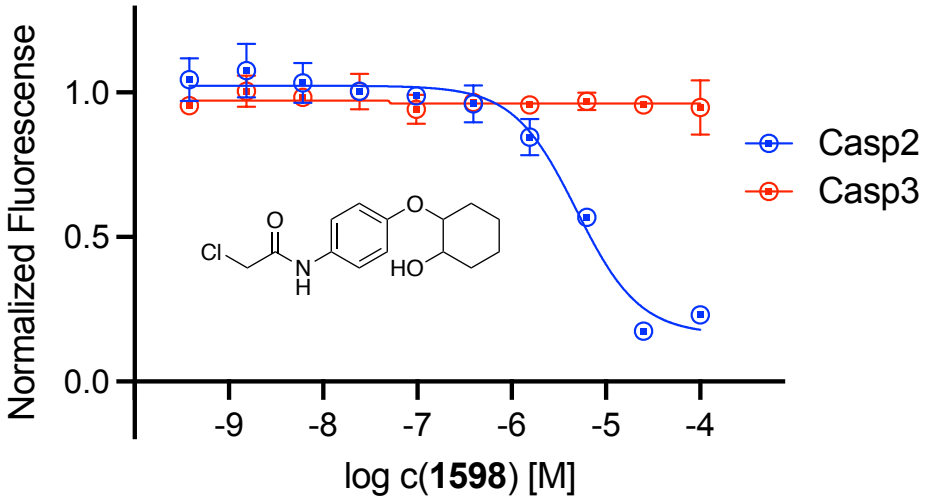

Figure S15. Concentration-response curve of **1598** at caspase-2 (blue) and caspase-3 (red) in the fluorometric enzyme assay. Data points represent mean values ± SD from representative experiments, each performed in duplicate.

Table S1. Enzyme inhibition activities from two-point and ten-point dose response screenings of selected electrophilic fragments at caspase-2 and caspase-3.

Cmpd.	Casp2 Inhibition at 12.5 µM [%][a]	Casp2 Inhibition at 6.25 µM [%][a]	Casp3 Inhibition at 125 µM [%][a]	Casp3 Inhibition at 62.5 µM [%][a]	pIC_{50} ± SEM[a] Casp2	N	Casp3	N	selectivity: IC_{50} (Casp3) / IC_{50} (Casp2)
13	72	46	14	0	5.28 ± 0.01	2	< 4.00	2	> 19
18	61	25	25	20	5.00 ± 0.02	2	< 4.00	1	> 10
31	62	41	86	76	5.11 ± 0.01	2	< 4.00	1	> 13
45	62	41	23	0	4.96 ± 0.01	2	< 4.00	1	> 9
67	62	45	71	77	5.06 ± 0.01	2	< 4.00	1	> 11
69	63	50	0	2	5.10 ± 0.01	2	< 4.00	1	> 12
77	74	48	42	13	5.19 ± 0.03	2	< 4.00	1	> 15
78	59	37	63	21	4.87 ± 0.05	2	< 4.00	1	> 7
79	60	38	46	16	5.02 ± 0.05	2	< 4.00	1	> 10
113	61	38	90	73	5.15 ± 0.03	2	< 4.00	1	> 14

124	60	50	9	3	5.24 ± 0.05	2	< 4.00	1	> 17
132	60	37	84	51	5.00 ± 0.06	2	< 4.00	1	> 10
178	59	31	86	40	4.95 ± 0.01	2	n.d.	-	-
210	59	37	31	6	4.90 ± 0.06	2	< 4.00	1	> 8
234	59	39	78	37	5.08 ± 0.01	2	< 4.00	1	> 12
246	65	45	80	33	5.06 ± 0.01	2	< 4.00	1	> 11
252	77	56	35	9	5.22 ± 0.02	2	< 4.00	1	> 17
285	72	49	73	29	5.22 ± 0.01	2	< 4.00	1	> 17
309	75	53	25	0	5.21 ± 0.01	2	< 4.00	1	> 16
708	83	70	81	48	5.36 ± 0.01	2	4.34 ± 0.16	2	10
995	67	45	5	4	5.05 ± 0.01	2	< 4.00	1	> 11
1072	77	55	32	8	5.24 ± 0.01	2	< 4.00	1	> 17
1094	80	61	58	15	5.33 ± 0.01	2	< 4.30	2	> 11
1111	87	72	86	58	5.47 ± 0.01	2	4.38 ± 0.13	2	12
1196	75	57	50	11	5.25 ± 0.03	2	< 4.00	1	> 18
1260	78	57	77	32	5.20 ± 0.03	2	< 4.00	1	> 16
1280	79	56	88	68	5.18 ± 0.01	2	< 4.00	1	> 15
1298	70	47	91	54	5.08 ± 0.04	2	< 4.00	1	> 12
1352	81	65	67	25	5.12 ± 0.01	2	< 4.00	1	> 13
1353	79	62	70	27	5.33 ± 0.02	2	4.51 ± 0.02	2	7
1355	68	56	5	2	5.21 ± 0.04	2	< 4.00	1	> 16
1356	80	63	53	12	5.19 ± 0.01	2	< 4.00	1	> 15
1393	80	60	22	3	5.28 ± 0.05	2	< 4.20	2	> 12
1399	72	51	0	1	5.11 ± 0.01	2	< 4.00	1	> 13
1428	84	63	2	2	5.05 ± 0.01	2	< 4.00	1	> 11

1439	64	46	8	10	5.05 ± 0.02	2	< 4.00	1	> 11
1513	63	44	49	12	4.99 ± 0.01	2	< 4.00	1	> 10
1553	75	54	81	38	5.18 ± 0.02	2	< 4.00	1	> 15
1580	65	43	19	10	5.01 ± 0.02	2	< 4.00	1	> 10
1586	75	56	31	5	5.16 ± 0.01	2	< 4.00	1	> 14
1627	84	62	44	13	5.15 ± 0.05	2	< 4.00	1	> 14
1652	78	38	5	3	4.94 ± 0.10	2	< 4.00	1	> 9
1695	60	40	18	4	4.59 ± 0.30	2	< 4.00	1	> 4
1753	80	47	23	2	4.99 ± 0.03	2	< 4.00	1	> 10
1776	75	58	59	15	5.19 ± 0.01	2	< 4.00	1	> 15
1783	78	66	85	74	5.15 ± 0.03	2	4.43 ± 0.14	2	5
1820	82	41	3	1	5.01 ± 0.02	2	< 4.00	1	> 10
1828	62	38	2	2	4.56 ± 0.05	2	< 4.00	1	> 4
1888	60	62	77	29	5.19 ± 0.01	2	< 4.00	1	> 15

[a]pIC_{50} values and single dose inhibition values were obtained based on measurements at 40 min. Data shown are mean values ± SEM of N independent experiments, each performed in duplicate. Data were analyzed by nonlinear regression and were best fitted to sigmoidal concentration−response curves (variable slope, four parameter fit). [b]k_{inact}/K_i values were calculated in two-steps by obtaining k_{obs} values first (a) Irreversible Inactivation and b) Two Step Irreversable Secondary Regression (Copeland 9.2)) and using kinetic data of at least four different inhibitor concentrations. n.d. = not determined.

Table S2. CNS Multiparameter Optimization (MPO) scores of compounds **17**, **46**, **97**, **118**, **196**, **1269**, and **1598**.

	17	**46**	**97**	**118**	**196**	**1269**	**1598**
MPO Score	5.8	5.5	5.1	5.5	5.8	6.0	5.5

CNS Multiparameter Optimization (MPO) score[1,2] (scale between 0 and 6) was calculated using six common physicochemical properties (MW, logP, logD at pH 7.4, TPSA, HBD, pKa of most basic center).

4. Target engagement study using MSPS

Target tethering to active site cysteine-320 (Cys320) at Casp2

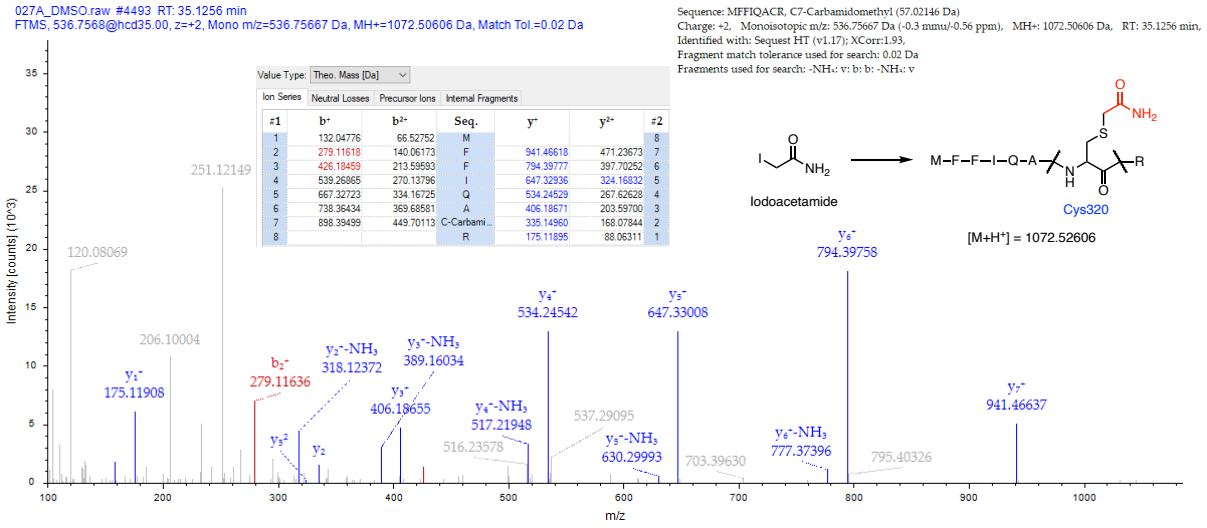

Figure S16. Mass spectrometry (MS) chromatogram of the adducted peptide MFFIQA**C**R with reference compound iodoacetamide (IAD). Sequence analysis by MS confirms fragment binding at active site Cys320. Columns b^+/b^{2+} and y^+/y^{2+} (single/double charge) represent the MS results of stepwise fragmentation of peptide "MFFIQA(C-fragment)R" (b: C-terminal fragmentation; y: N-terminal fragmentation).

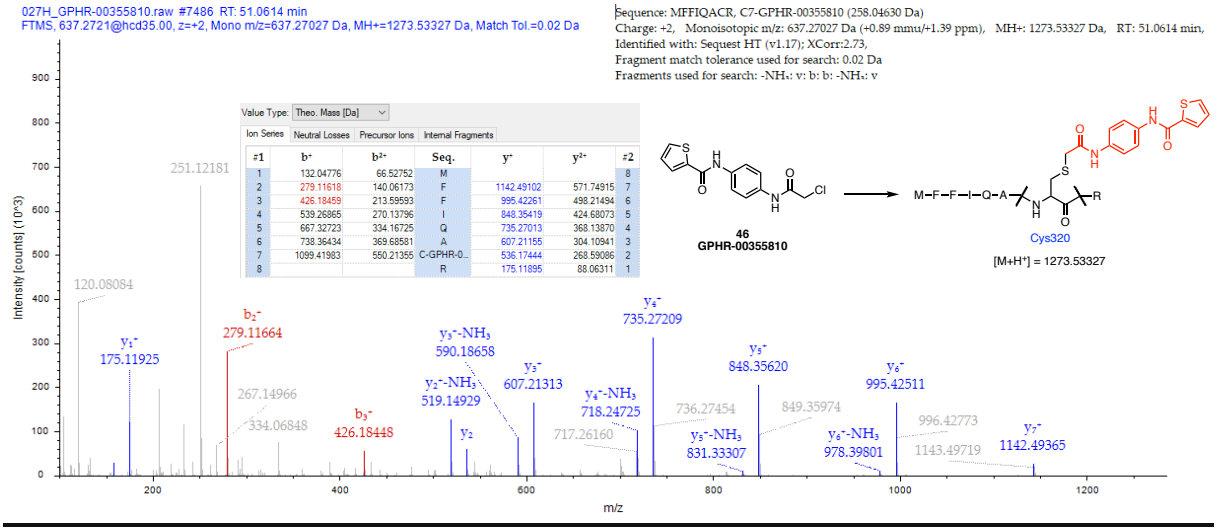

Figure S17. Mass spectrometry (MS) chromatogram of the adducted peptide MFFIQA**C**R with electrophilic fragment **46** (GPHR-00355810). Sequence analysis by MS confirms fragment binding at active site Cys320. Columns b^+/b^{2+} and y^+/y^{2+} (single/double charge) represent the MS results of stepwise fragmentation of peptide "MFFIQA(C-fragment)R" (b: C-terminal fragmentation; y: N-terminal fragmentation).

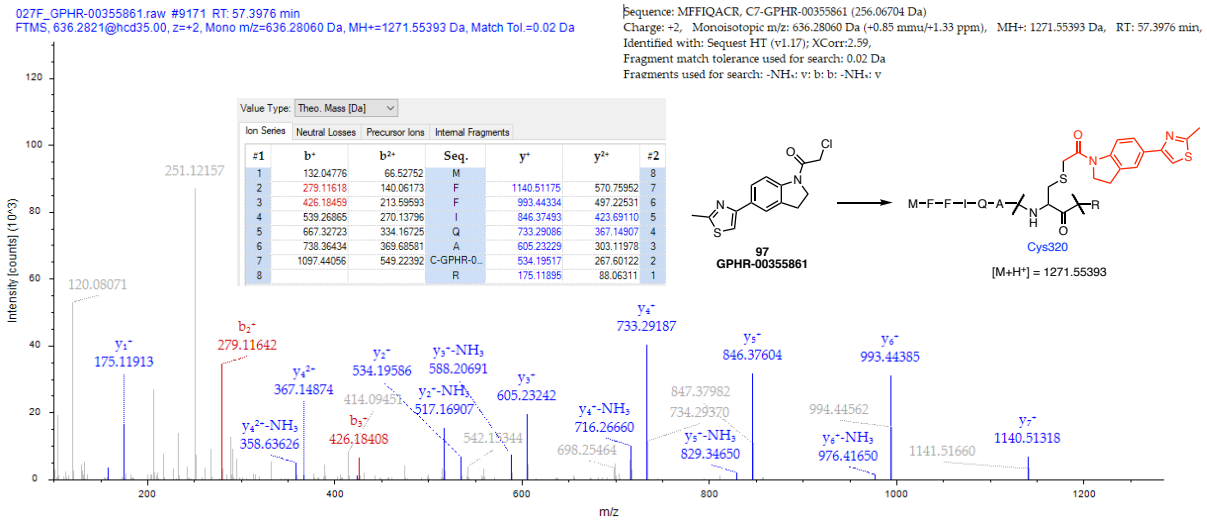

Figure 18. Mass spectrometry (MS) chromatogram of the adducted peptide MFFIQA**C**R with electrophilic fragment **97** (GPHR-00355861). Sequence analysis by MS confirms fragment binding at active site Cys320. Columns b^+/b^{2+} and y^+/y^{2+} (single/double charge) represent the MS results of stepwise fragmentation of peptide "MFFIQA(C-fragment)R" (b: C-terminal fragmentation; y: N-terminal fragmentation).

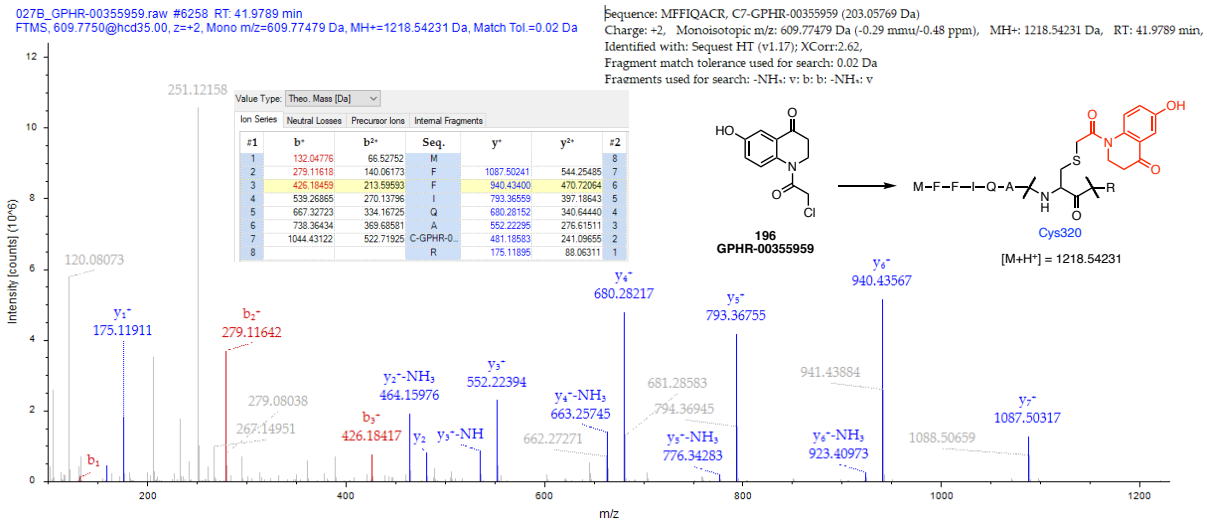

Figure S19. Mass spectrometry (MS) chromatogram of the adducted peptide MFFIQA**C**R with electrophilic fragment **196** (GPHR-00355959). Sequence analysis by MS confirms fragment binding at active site Cys320. Columns b^+/b^{2+} and y^+/y^{2+} (single/double charge) represent the MS results of stepwise fragmentation of peptide "MFFIQA(C-fragment)R" (b: C-terminal fragmentation; y: N-terminal fragmentation).

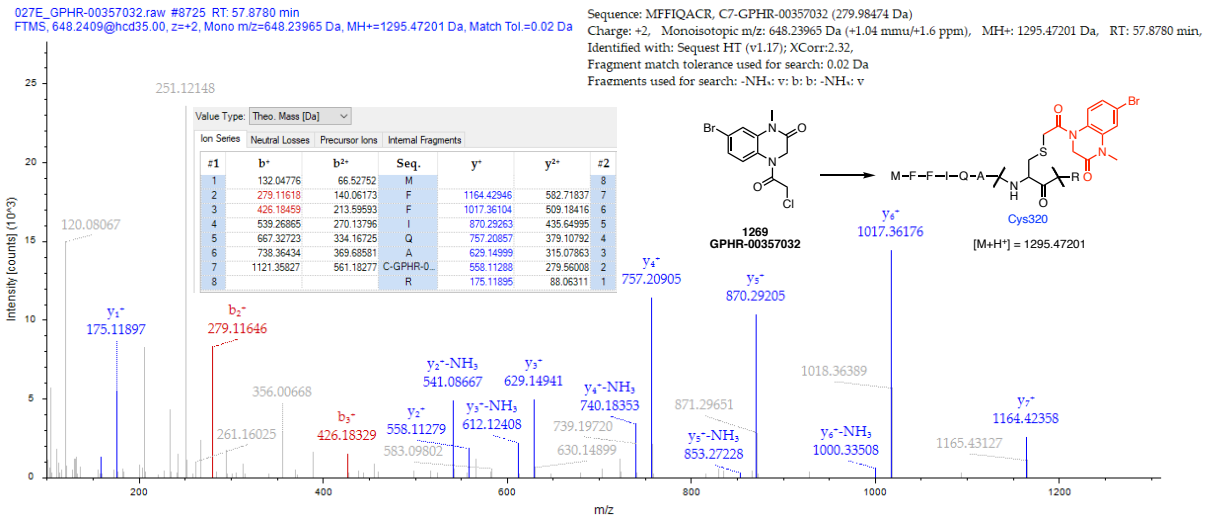

Figure S20. Mass spectrometry (MS) chromatogram of the adducted peptide MFFIQA**C**R with electrophilic fragment **1269** (GPHR-00357032). Sequence analysis by MS confirms fragment binding at active site Cys320. Columns b^+/b^{2+} and y^+/y^{2+} (single/double charge) represent the MS results of stepwise fragmentation of peptide "MFFIQA(C-fragment)R" (b: C-terminal fragmentation; y: N-terminal fragmentation).

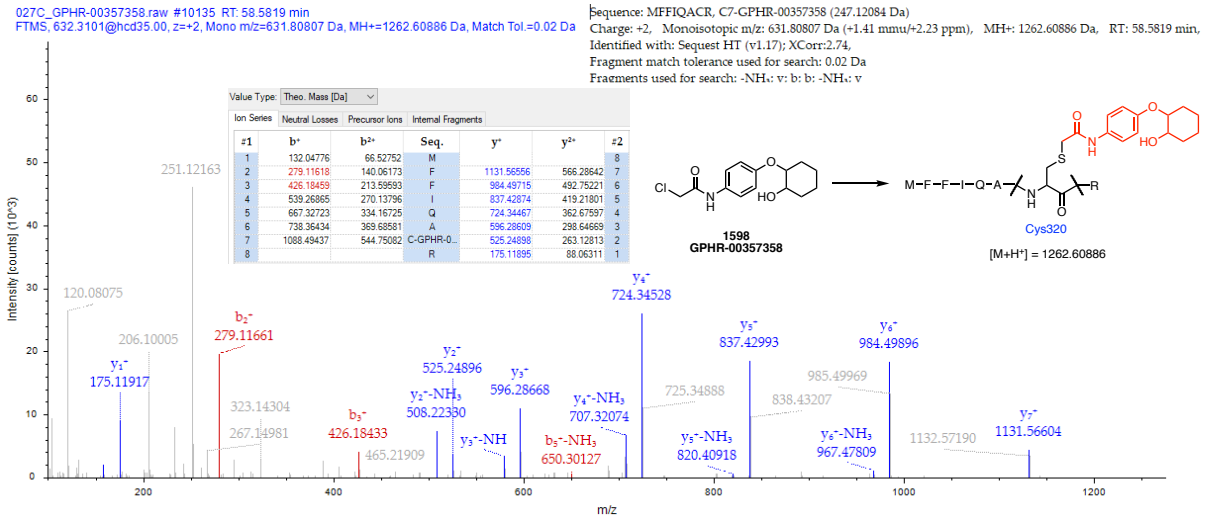

Figure S21. Mass spectrometry (MS) chromatogram of the adducted peptide MFFIQA**C**R with electrophilic fragment **1598** (GPHR-00357358). Sequence analysis by MS confirms fragment binding at active site Cys320. Columns b^+/b^{2+} and y^+/y^{2+} (single/double charge) represent the MS results of stepwise fragmentation of peptide "MFFIQA(C-fragment)R" (b: C-terminal fragmentation; y: N-terminal fragmentation).

Table S3. Summary of key peaks from the MS study in association with tested hit compounds **17**, **46**, **97**, **196**, **1269**, and **1598** or reference compound iodoacetamide.

cmpd.	**17**	**46**	**97**	**196**
$[M+H]^+$	1203.54259	1273.53327	1271.55393	1218.54231
cmpd.	**1269**	**1598**	**IAD**	
$[M+H]^+$	1295.47201	1262.60886	1072.52606	

Off-target tethering to other cysteines at Casp2

17/GPHR-00355781
Observed as a single modification of the indicated peptide, i.e. peptide only has Cys modification:

- Cys244, LLGYDVHVL**C**DQTAQEMQEK
- Cys399, A**C**DMHVADMLVK
- Cys270, VTDS**C**IVALLSHGVEGAIYGVDGK

Also, observed but only in combination with other modifications like carbamidomethyl and/or oxidation, i.e. peptide has Cys modification and oxidation:

- Cys429, **C**KEMSEYCSTLCR
- Cys436, CKEMSEY**C**STLCR
- Cys370, SDMICGYA**C**LK

46/GPHR-00355810
Observed as a single modification of the indicated peptide, i.e. peptide only has Cys modification:

- Cys244, LLGYDVHVL**C**DQTAQEMQEK
- Cys399, A**C**DMHVADMLVK
- Cys270, VTDS**C**IVALLSHGVEGAIYGVDGK

Also, observed but only in combination with other modifications like carbamidomethyl and/or oxidation, i.e. peptide has Cys modification and oxidation:

- Cys429, **C**KEMSEYCSTLCR
- Cys436, CKEMSEY**C**STLCR
- Cys440, CKEMSEYCSTL**C**R
- Cys366, SDMI**C**GYACLK
- Cys370, SDMICGYA**C**LK

97/GPHR-00355861
Observed as a single modification of the indicated peptide, i.e. peptide only has Cys modification:

- Cys244, LLGYDVHVL**C**DQTAQEMQEK
- Cys399, A**C**DMHVADMLVK
- Cys270, VTDS**C**IVALLSHGVEGAIYGVDGK

Also, observed but only in combination with other modifications like carbamidomethyl and/or oxidation, i.e. peptide has Cys modification and oxidation:

- Cys429, **C**KEMSEYCSTLCR
- Cys436, CKEMSEY**C**STLCR
- Cys440, CKEMSEYCSTL**C**R
- Cys366, SDMI**C**GYACLK
- Cys370, SDMICGYA**C**LK

Also, observed double labeling of a peptide with the chloroacetamide; also in combination with other modifications like carbamidomethyl and/or oxidation:

- Cys429 and Cys436, **C**KEMSEY**C**STLCR

196/GPHR-00355959
Observed as a single modification of the indicated peptide, i.e. peptide only has Cys modification:

- Cys244, LLGYDVHVL**C**DQTAQEMQEK
- Cys399, A**C**DMHVADMLVK
- Cys270, VTDS**C**IVALLSHGVEGAIYGVDGK
- Cys305, LLQLQEVFQLFDNAN**C**PSLQNKPK

Also, observed but only in combination with other modifications like carbamidomethyl and/or oxidation, i.e. peptide has Cys modification and oxidation:

- Cys429, **C**KEMSEYCSTLCR
- Cys436, CKEMSEY**C**STLCR
- Cys440, CKEMSEYCSTL**C**R
- Cys366, SDMI**C**GYACLK
- Cys370, SDMICGYA**C**LK

Also, observed double labeling of a peptide with the chloroacetamide; also in combination with other modifications like carbamidomethyl and/or oxidation:

- Cys429 and Cys436, **C**KEMSEY**C**STLCR

1269/GPHR-00357032;
Observed as a single modification of the indicated peptide, i.e. peptide only has Cys modification:

- Cys270, VTDS**C**IVALLSHGVEGAIYGVDGK

Also, observed but only in combination with other modifications like carbamidomethyl and/or oxidation, i.e. peptide has Cys modification and oxidation:

- Cys436, CKEMSEY**C**STLCR
- Cys399, A**C**DMHVADMLVK

1598/GPHR-00357358
Observed as a single modification of the indicated peptide, i.e. peptide only has Cys modification:

- Cys244, LLGYDVHVL**C**DQTAQEMQEK
- Cys399, A**C**DMHVADMLVK
- Cys270, VTDS**C**IVALLSHGVEGAIYGVDGK

Also, observed but only in combination with other modifications like carbamidomethyl and/or oxidation, i.e. peptide has Cys modification and oxidation:

- Cys429, **C**KEMSEYCSTLCR
- Cys436, CKEMSEY**C**STLCR
- Cys440, CKEMSEYCSTL**C**R

5. GSH-Glo™ Glutathione and CellTiter-Glo™ Luminescent Cell Viability Assay

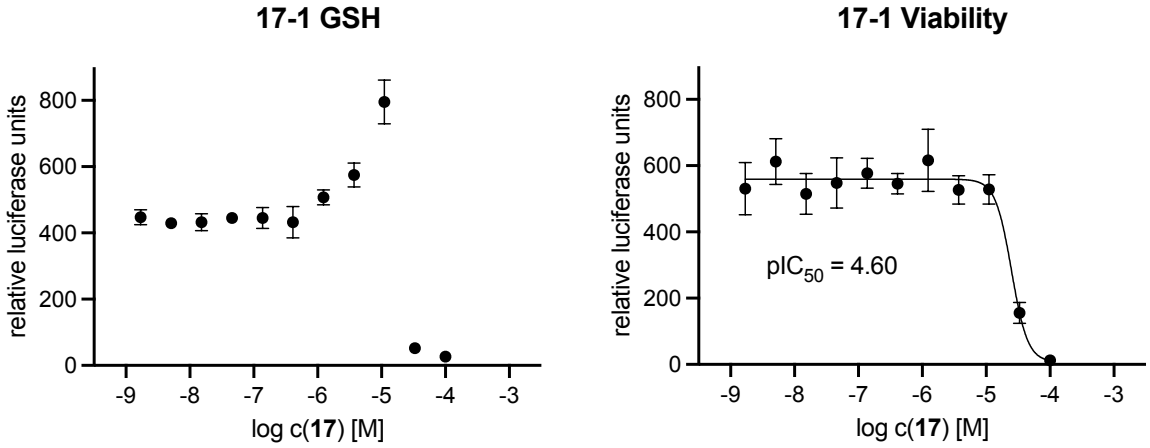

Figure S22. Concentration-response curves of **17** (N=1 in quadruplicates) in the GSH-Glo™ Glutathione Assay (left) and CellTiter-Glo™ Luminescent Cell Viability Assay (right).

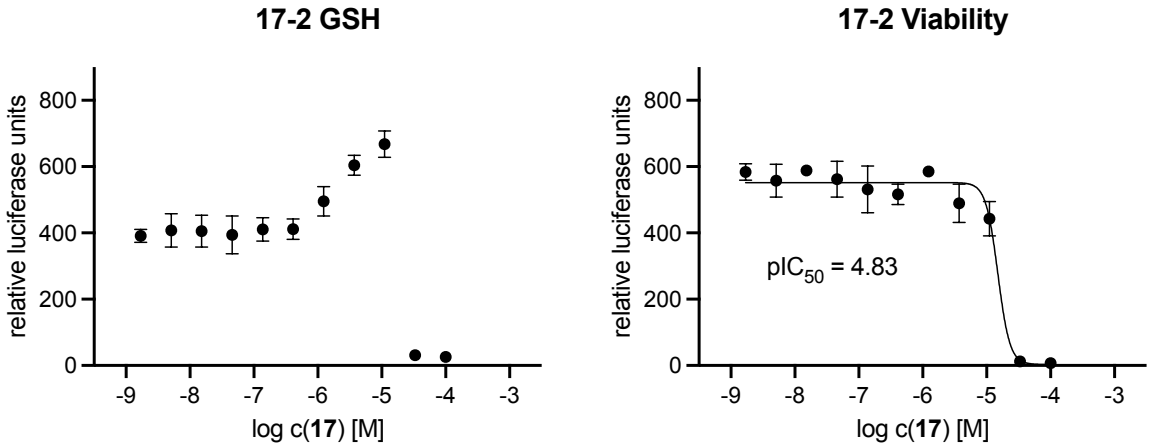

Figure S23. Concentration-response curves of **17** (N=2 in quadruplicates) in the GSH-Glo™ Glutathione Assay (left) and CellTiter-Glo™ Luminescent Cell Viability Assay (right).

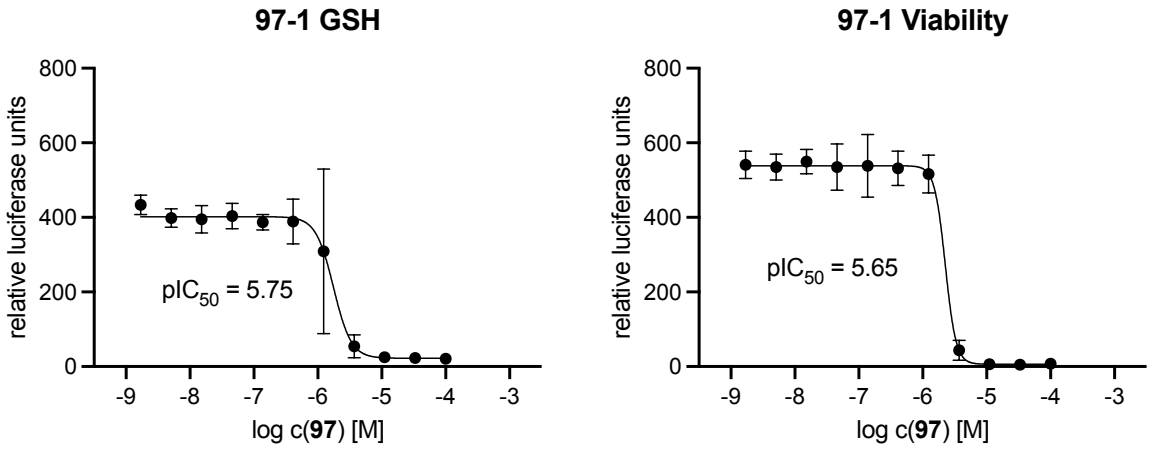

Figure S24. Concentration-response curves of **97** (N=1 in quadruplicates) in the GSH-Glo™ Glutathione Assay (left) and CellTiter-Glo™ Luminescent Cell Viability Assay (right).

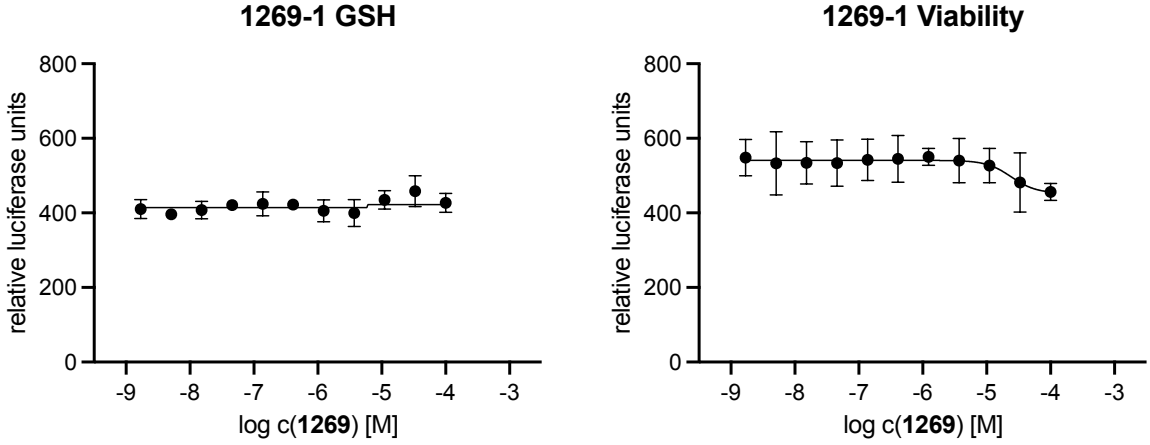

Figure S25. Concentration-response curves of **1269** (N=1 in quadruplicates) in the GSH-Glo™ Glutathione Assay (left) and CellTiter-Glo™ Luminescent Cell Viability Assay (right).

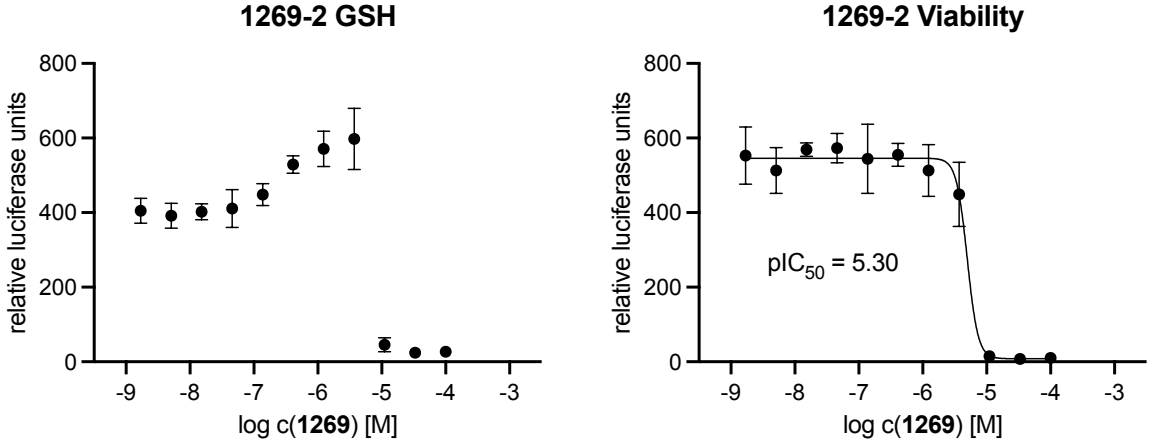

Figure S26. Concentration-response curves of **1269** (N=2 in quadruplicates) in the GSH-Glo™ Glutathione Assay (left) and CellTiter-Glo™ Luminescent Cell Viability Assay (right).

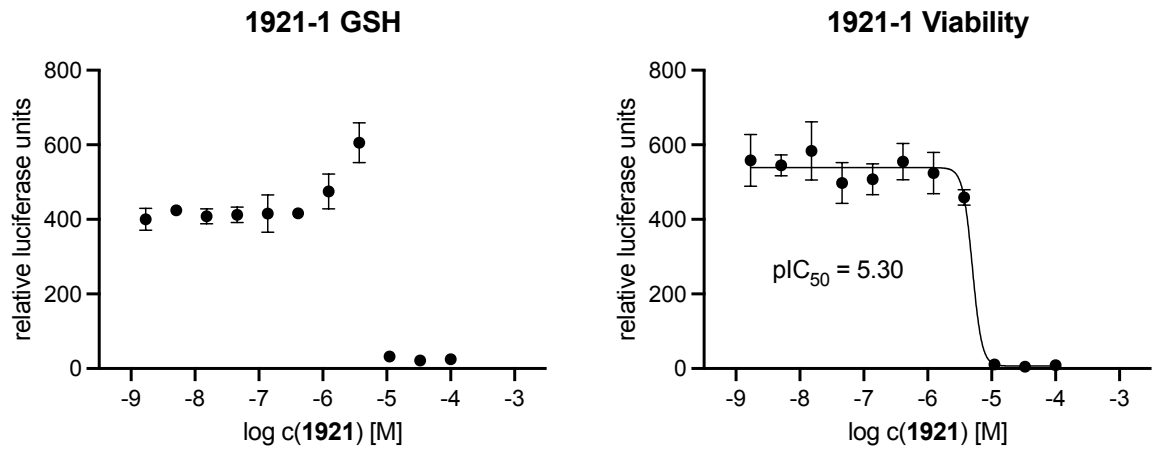

Figure S27. Concentration-response curves of **1921** (N=1 in quadruplicates) in the GSH-Glo™ Glutathione Assay (left) and CellTiter-Glo™ Luminescent Cell Viability Assay (right).

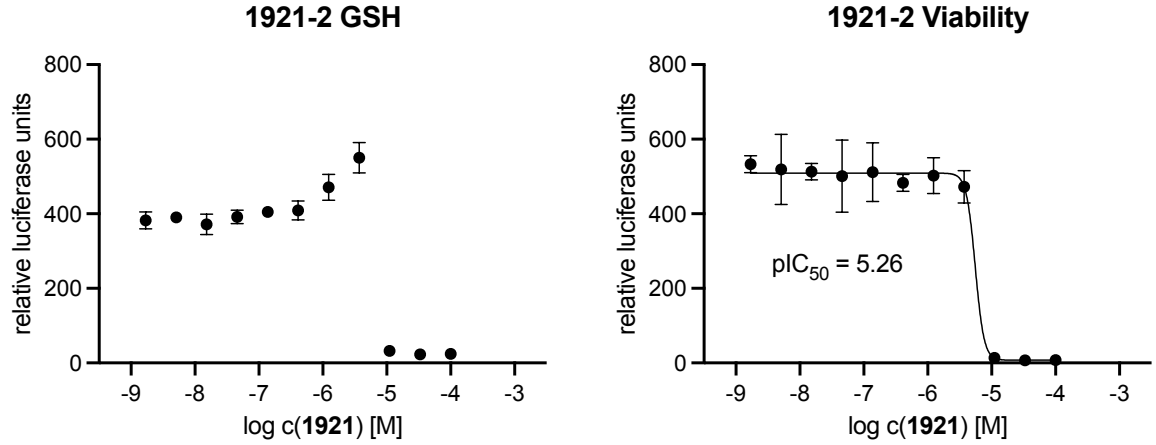

Figure S28. Concentration-response curves of **1921** (N=2 in quadruplicates) in the GSH-Glo™ Glutathione Assay (left) and CellTiter-Glo™ Luminescent Cell Viability Assay (right).

6. Synthesis for hit validation

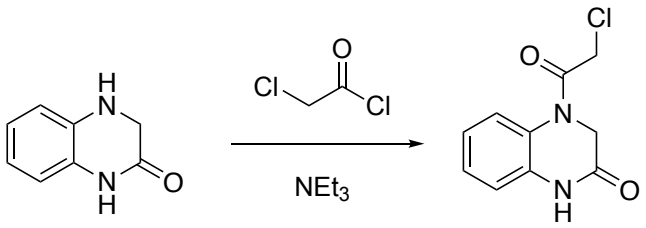

17*

4-(2-Chloroacetyl)-3,4-dihydroquinoxalin-2(1H)-one (17*): 2-Chloroacetyl chloride (305 mg, 2.70 mmol) was slowly added to a suspension of 3,4-dihydroquinoxalin-2(1H)-one (200 mg, 1.350 mmol) and TEA (205 mg, 2.03 mmol) in anhydrous DCM (5 mL) at 0 °C. The reaction mixture was stirred at 0 °C for 1.5 h and at room temperature for 3 h. The reaction mixture was added to saturated aqueous $NaHCO_3$ aqueous solution and then extracted with ethyl acetate and washed with saturated aqueous NaCl solution, dried over $MgSO_4$, and concentrated under reduced pressure. The residue was washed with water and dried to yield the desired product. The crude mixture was diluted with DMSO and purified by reverse phase chromatography (Method Acidic Standard Gradient) to afford as a TFA salt,

4-(2-Chloroacetyl)-3,4-dihydroquinoxalin-2(1H)-one: LCMS: *m/z* $(M+H)^+$ = 225.0, retention time = 1.57 min. ^1H NMR (400 MHz, d_6 DMSO) δ 10.72 (s, 1H), 7.55 (d, *J* = 7.9 Hz, 1H), 7.21 (t, *J* = 7.7 Hz, 1H), 7.03 (ddd, *J* = 15.0, 7.7, 1.5 Hz, 2H), 4.54 (s, 2H), 4.34 (s, 2H). HRMS (ESI) m/z $(M+H)^+$ calculated for molecular formula $C_{10}H_9ClN_2O_2$; 224.0334 found 224.0353.

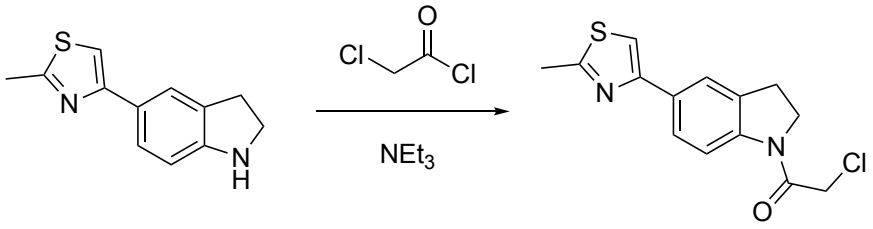

97**

2-Chloro-1-(5-(2-methylthiazol-4-yl)indolin-1-yl)ethan-1-one (97):** 2-Chloroacetyl chloride (44.2 µl, 0.555 mmol) was slowly added to a suspension of 4-(indolin-5-yl)-2-methylthiazole (100 mg, 0.462 mmol) and TEA (97 µl, 0.69 mmol) in anhydrous DCM (5 mL) at 0 °C. The reaction mixture was stirred at 0 °C for 1.5 h and at room temperature for 3 h. The reaction mixture was added to a saturated aqueous $NaHCO_3$ solution and then extracted with ethyl acetate and washed with saturated aqueous

NaCl solution, dried over $MgSO_4$, and concentrated under reduced pressure. The residue was washed with water and dried to yield the desired product. The crude mixture was diluted with DMSO and purified by reverse phase chromatography (Method Acidic Standard Gradient) to afford as a TFA salt,

2-Chloro-1-(5-(2-methylthiazol-4-yl)indolin-1-yl)ethan-1-one : LCMS: *m/z* $(M+H)^+$ = 293.0, retention time = 1.95 min. ^1H NMR (400 MHz, d_6 DMSO) δ 8.04 (d, *J* = 8.4 Hz, 1H), 7.84 – 7.73 (m, 3H), 4.53 (s, 2H), 4.15 (t, *J* = 8.4 Hz, 2H), 3.20 (t, *J* = 8.4 Hz, 2H), 2.68 (s, 3H). HRMS (ESI) m/z $(M+H)^+$ calculated for molecular formula $C_{14}H_{13}ClN_2OS$; 292.0425 found 292.0437.

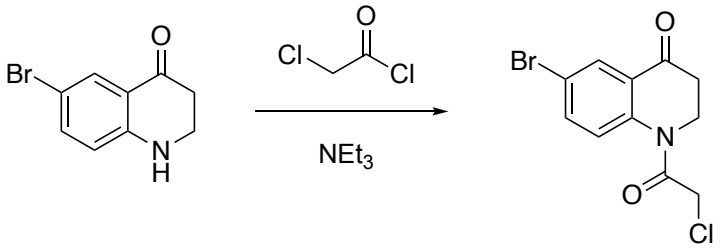

1921

6-Bromo-1-(2-chloroacetyl)-2,3-dihydroquinolin-4(1H)-one (1921): 2-Chloroacetyl chloride (42.3 µl, 0.531 mmol) was slowly added to a suspension of 6-bromo-2,3-dihydroquinolin-4(1H)-one (100 mg, 0.442 mmol) and TEA (92 µl, 0.66 mmol) in anhydrous DCM (5 mL) at 0 ^oC. The reaction mixture was stirred at 0 ^oC for 1.5 h and at room temperature for 3 h. The reaction mixture was added to saturated aqueous $NaHCO_3$ solution and then extracted with ethyl acetate and washed with saturated aqueous NaCl solution, dried over $MgSO_4$, and concentrated under reduced pressure. The residue was washed with water and dried to yield the desired product. The crude mixture was diluted with DMSO and purified by reverse phase chromatography (Method Acidic Standard Gradient) to afford as a TFA salt,

6-Bromo-1-(2-chloroacetyl)-2,3-dihydroquinolin-4(1H)-one: LCMS: *m/z* $(M+H)^+$ = 303.0 retention time = 1.92 min. ; ^1H NMR (400 MHz, d_6 DMSO) δ 7.92 (d, *J* = 2.3 Hz, 1H), 7.84 – 7.73 (m, 2H), 4.70 (s, 2H), 4.11 (t, *J* = 6.1 Hz, 2H), 2.87 – 2.79 (m, 2H); HRMS (ESI) m/z $(M+H)^+$ calculated for molecular formula $C_{11}H_9BrClNO_2$; 303.9556 found 303.9591.

7. NMR spectra and RP-HPLC chromatograms of 97* and 1269*

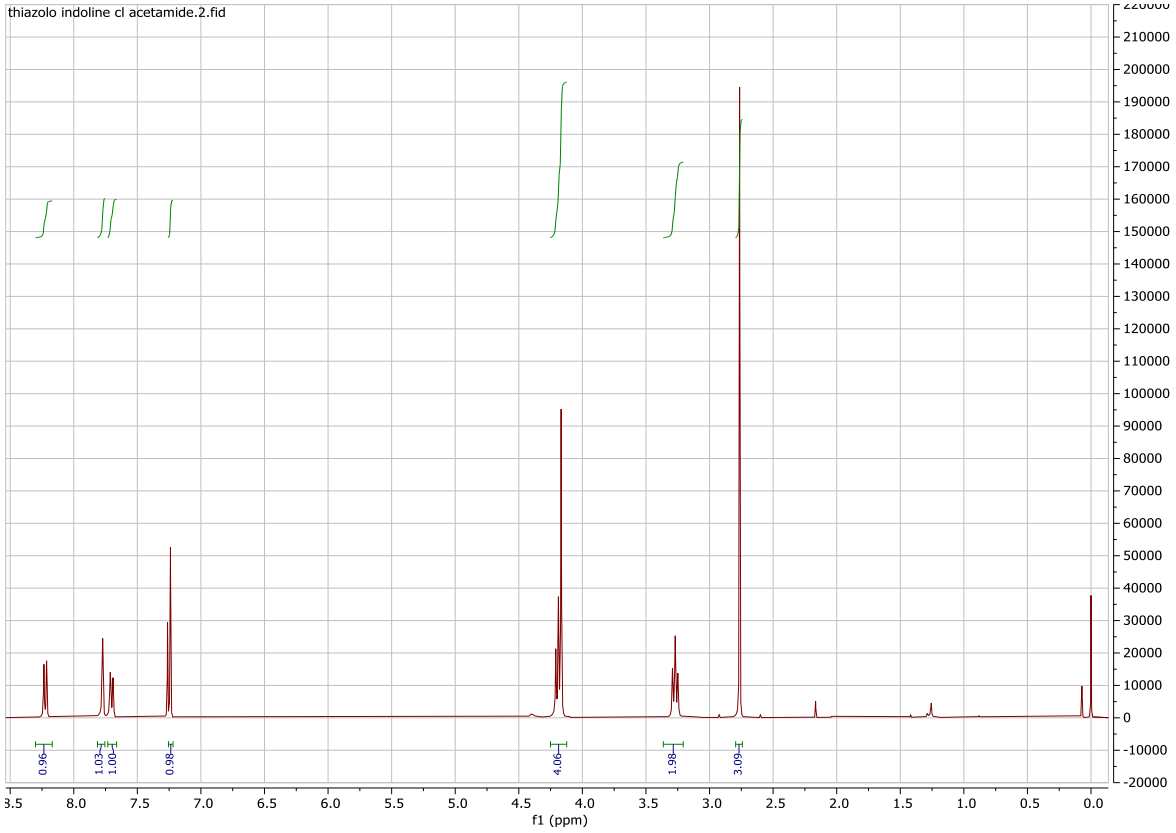

Figure S29. ^{1}H NMR spectrum (400 MHz, $CDCl_3$) of compound **97***.

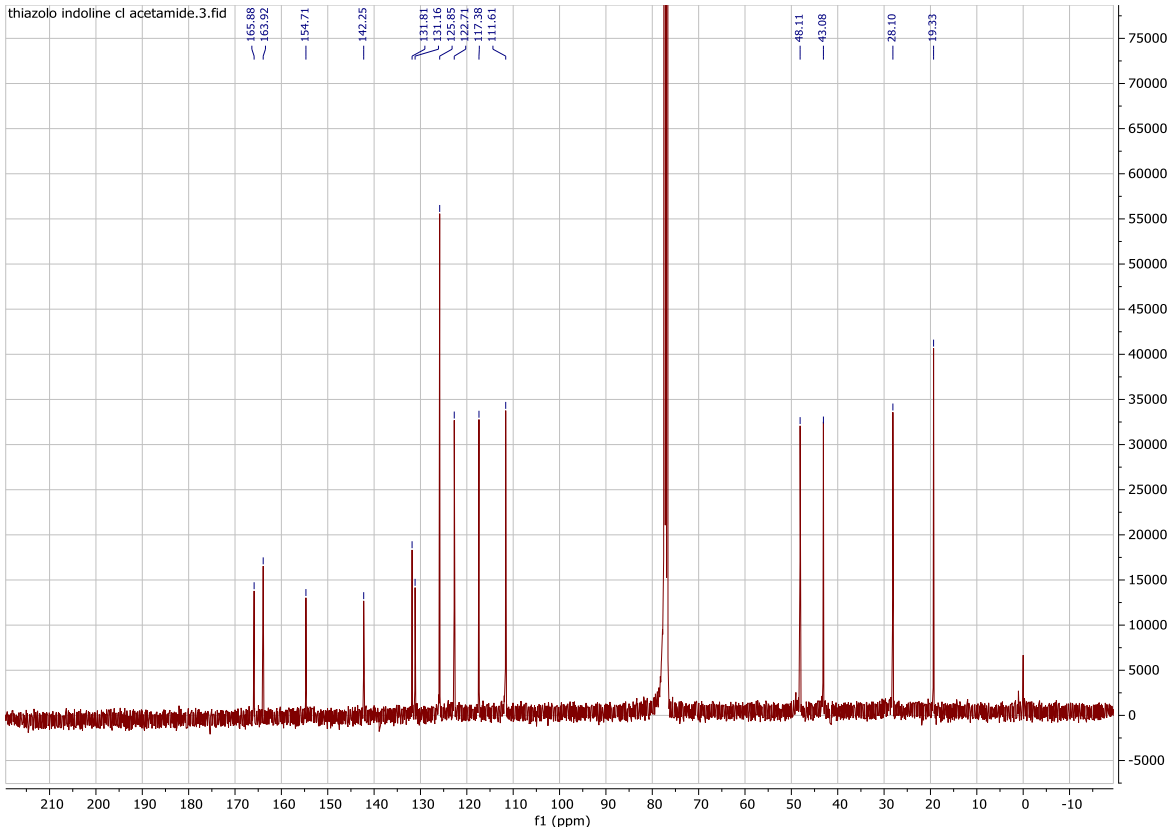

Figure S30. ^{13}C NMR spectrum (101 MHz, $CDCl_3$) of compound **97***.

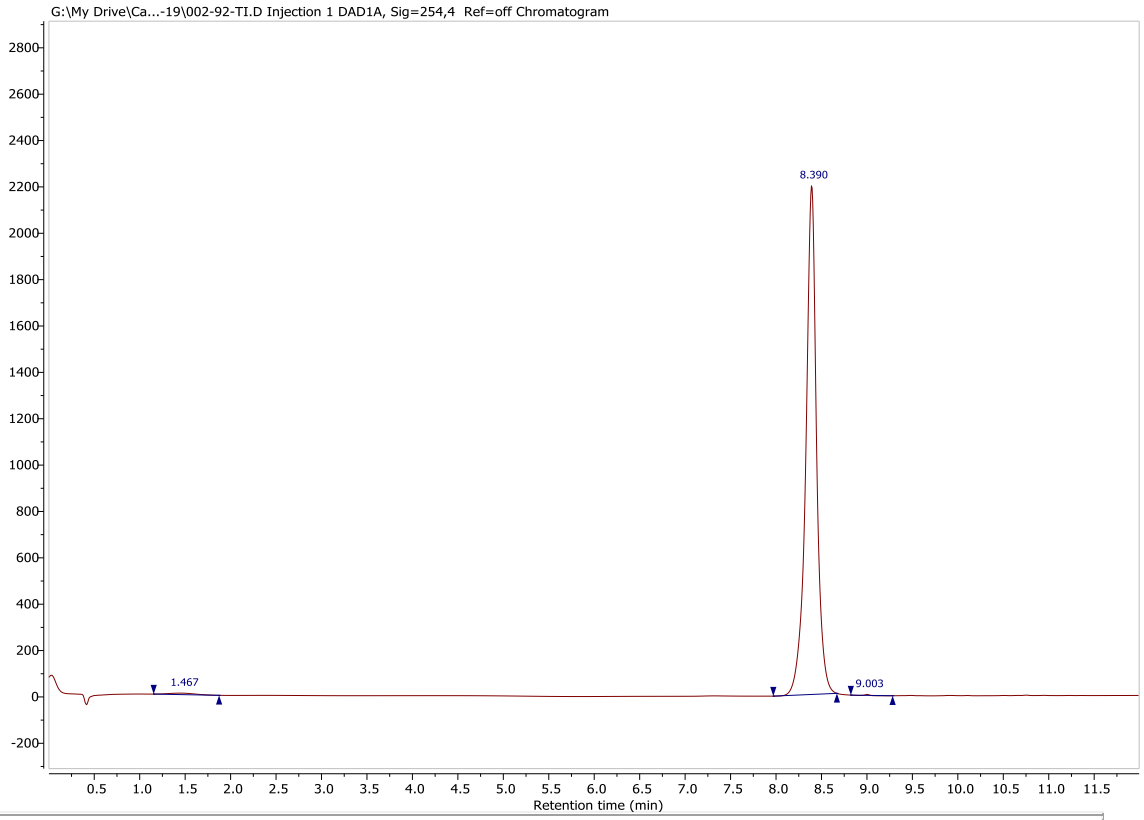

	RT	Area	Total Area %	Start time	End time
1	1.467	315.940	0.70	1.154	1.874
2	8.390	45111.995	99.25	7.970	8.670
3	9.003	26.392	0.06	8.823	9.283

Figure S31. RP-HPLC analysis (purity control) of compound **97***.

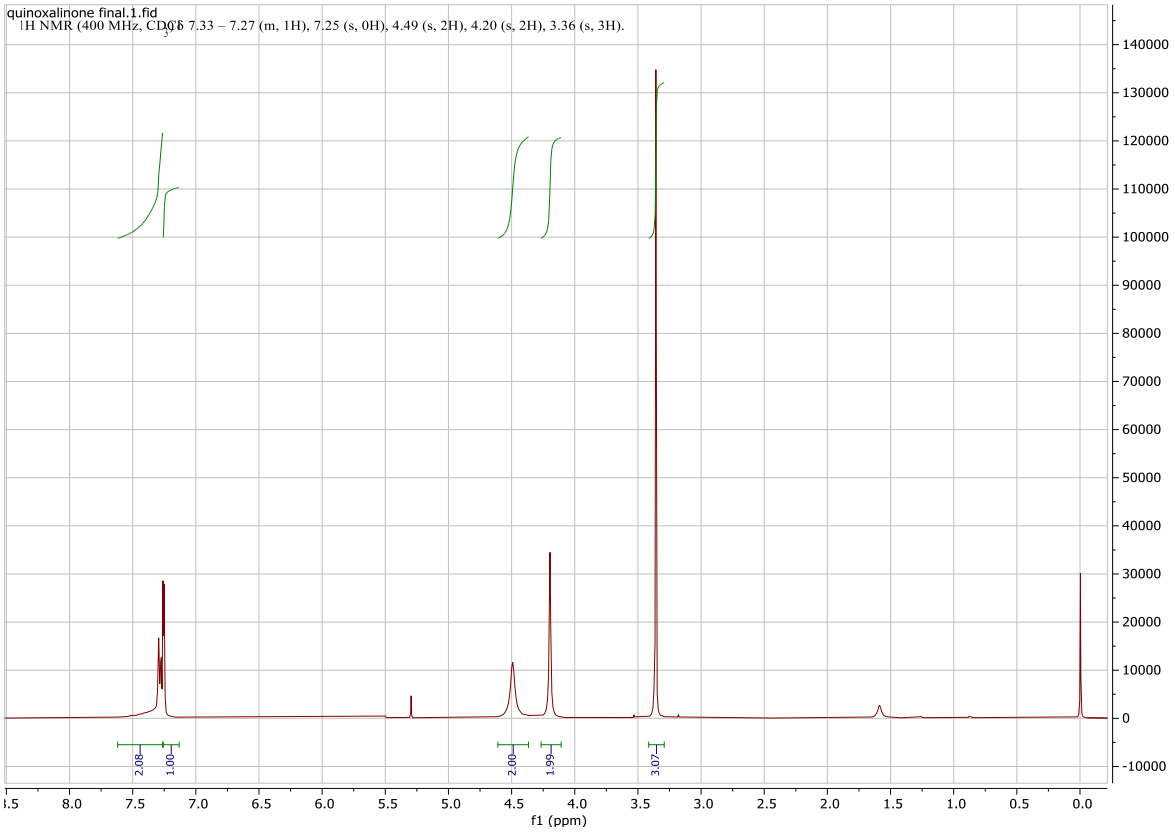

Figure S32. ^{1}H NMR spectrum (400 MHz, $CDCl_3$) of compound **1269***.

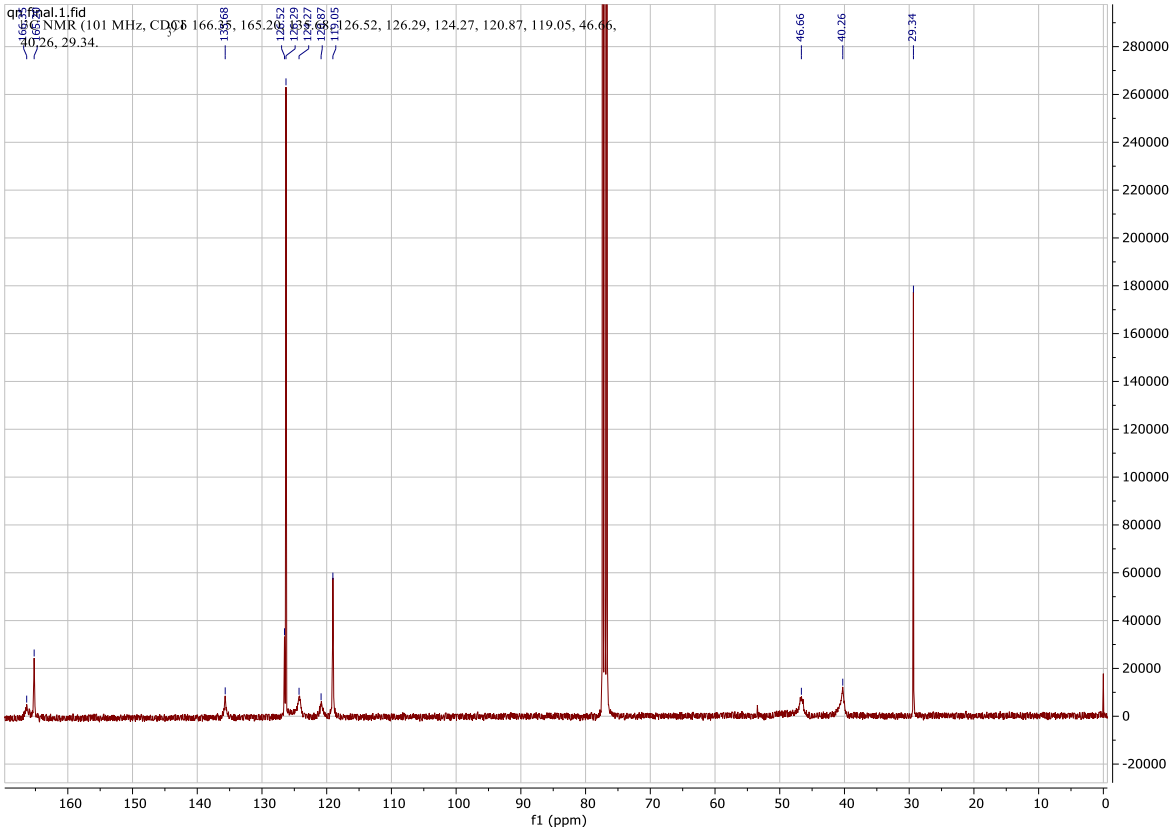

Figure S33. ^{13}C NMR spectrum (101 MHz, $CDCl_3$) of compound **1269***.

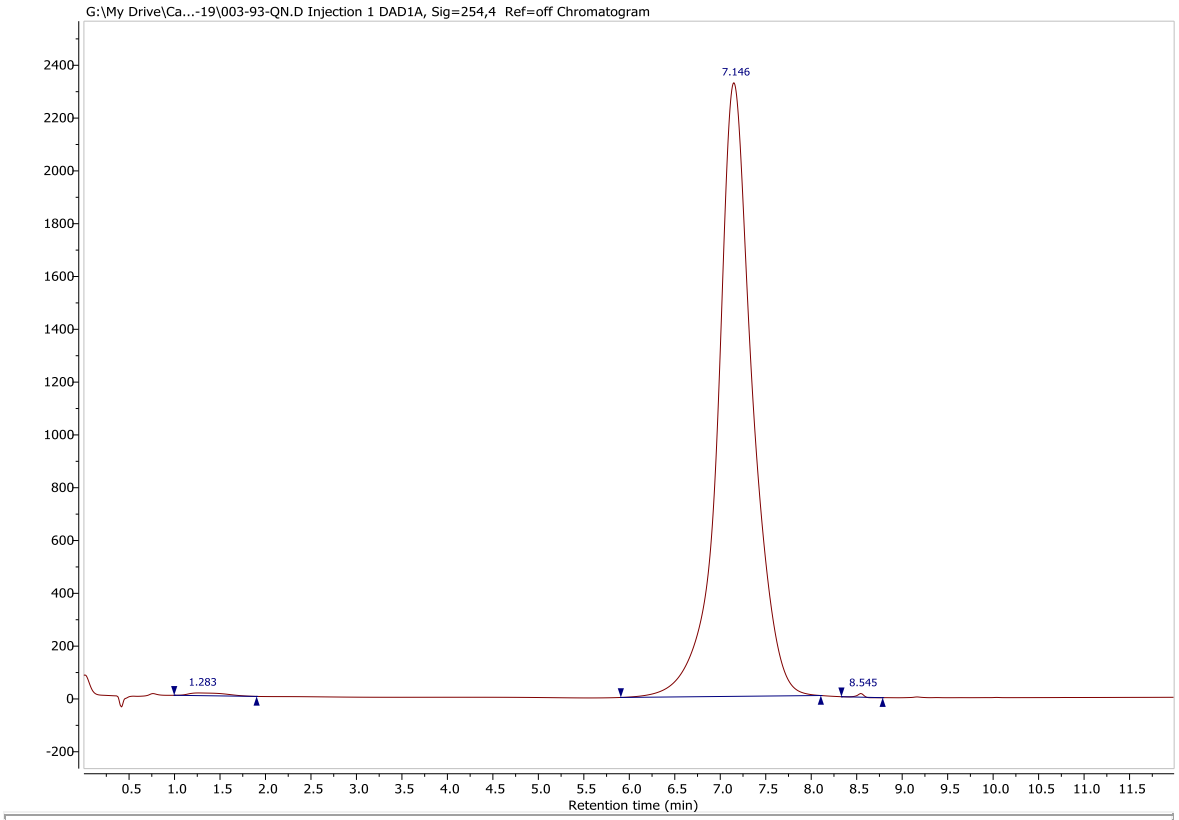

	RT	Area	Total Area %	Start time	End time
1	1.283	740.490	0.48	0.996	1.902
2	7.146	154841.747	99.42	5.907	8.106
3	8.545	161.768	0.10	8.332	8.785

Figure S34. RP-HPLC analysis (purity control) of compound **1269***.

8. References

[1] T.T. Wager, X. Hou, P.R. Verhoest, A. Villalobos, Moving beyond Rules: The Development of a Central Nervous System Multiparameter Optimization (CNS MPO) Approach To Enable Alignment of Druglike Properties, ACS Chemical Neuroscience. 1 (2010) 435–449. https://doi.org/10.1021/cn100008c.

[2] T.T. Wager, X. Hou, P.R. Verhoest, A. Villalobos, Central Nervous System Multiparameter Optimization Desirability: Application in Drug Discovery, ACS Chemical Neuroscience. 7 (2016) 767–775. https://doi.org/10.1021/acschemneuro.6b00029.